## References and Notes

(1) Nagoya University, Department of Synthetic Chemistry, Forocho, Chikusa-ku, Nagoya, Japan.
(2) G. DiPaola-Baranyi and J. E. Guillet, *Macromolecules*, 11, 228 (1978).
(3) G. DiPaola-Baranyi, J. E. Guillet, J. Klein, and H.-E. Jeberien, *J. Chromatogr.*, 166, 349 (1978).
(4) J. H. Hildebrand and R. L. Scott, "The Solubility of Nonelectrolytes", 3rd ed., Reinhold, New York, 1950.
(5) P. J. Flory, "Principles of Polymer Chemistry", Cornell University Press, Ithaca, N. Y., 1953.
(6) D. Patterson, *Rubber Chem. Technol.*, 40, 1 (1967).
(7) M. L. Huggins, *Ann. N.Y. Acad. Sci.*, 43, 1 (1942).
(8) R. L. Scott and M. Magat, *J. Chem. Phys.*, 13, 172 (1945); *J. Polym. Sci.*, 4, 555 (1949).
(9) G. M. Bristow and W. F. Watson, *Trans Faraday Soc.*, 54, 1731 (1958); 54, 1742 (1958).
(10) D. R. Dreisbach, *Adv. Chem. Ser.*, No. 15 (1955); No. 22 (1959); No. 29 (1961).
(11) "Encyclopedia of Polymer Science and Technology", Vol. 6, Wiley-Interscience, New York, 1971.
(12) J. Brandrup and E. H. Immergut, Ed., "Polymer Handbook", Interscience, New York, 1966.
(13) S. Newman, *J. Polym. Sci.*, 47, 111 (1960).


# Triplet Energy Migration in Polymer Photochemistry. A Model for the Photodegradation of Poly(phenyl vinyl ketone) in Solution


**M. V. Encinas, K. Funabashi, and J. C. Scaiano***

*Radiation Laboratory,[1] University of Notre Dame, Notre Dame, Indiana 46556.*

*Received May 31, 1979*


ABSTRACT: Plots of the progress of the degradation of poly(phenyl vinyl ketone) as a function of irradiation time are nonlinear; the effect is the result of triplet quenching by unsaturated end groups generated in the reaction. The process is intramolecular, and from a study of polymers of different initial chain length and application of random walk theory for a one-dimensional lattice it is possible to determine the frequency of triplet energy hopping; the value obtained was $\sim 1 \times 10^{12}$ $s^{-1}$ at 30 °C in benzene. Poly(phenyl vinyl ketone) has a critical chain length of 750 units, this being the average number of chromophores "visited" by the excitation during the triplet lifetime.


The transfer of electronic energy is a process of importance in numerous systems.[2-4] The migration of electronic energy between chromophores of the same type has received attention in solution and in the solid state.[5-9] While singlet energy transfer can occur by several mechanisms, triplet–triplet transfer can only occur by the exchange mechanism, which requires the donor and acceptor groups to be close enough to allow significant overlap of their electron clouds.[5,6]

Energy migration between identical groups is of importance in crystals, glasses, and polymer systems in general. Transfers between truly identical chromophores are virtually impossible to study because the energy transfer process does not lead to an easily observable phenomenon, and most studies make use of small differences between the donor and acceptor molecule. For example, in the case of polymers, the donor and acceptor may differ only in that one of them will be closer to the end of the chain, while they are identical in all other respects. Energy migration of this type is often responsible for the occurrence of chemical or physical processes at a considerable distance from the original excitation site. This phenomenon has important practical implications in the field of photostabilizers, some of which work on the principle of excitation migration toward a suitable energy sink;[10] processes of this type can only be of importance if migration "funnels" the energy toward the sink.

The photochemistry of polymers in the presence of "impurity" traps has been the subject of several studies in films and glasses,[2,11-17] but little is known about the behavior in solution.[18-26]

Poly(phenyl vinyl ketone), PPVK, has been the subject of numerous photochemical studies.[16a,20,21,23-30] The polymer undergoes cleavage via the Norrish type II reaction from the triplet manifold.[20,23]

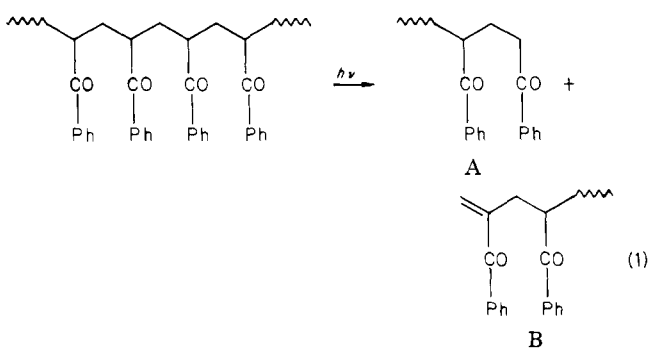


(1)

When the degradation process is monitored as a function of the irradiation time, the corresponding plot shows significant curvature (Figure 1). This curvature becomes quite evident at extremely low conversions, that is, under conditions where the number of chromophores which have participated in reaction 1 is only a small fraction of the total number of chromophores, typically ~0.1%. Quite clearly, the effect cannot be attributed to the depletion of reactive sites, nor is it the result of UV screening by products or impurities in the polymer (see Results Section). This unusual effect attracted our attention to the problem, which we propose results from intramolecular triplet quenching by $\alpha,\beta$-unsaturated carbonyl chromophores of the type shown in fragment B in reaction 1. These groups behave as extremely efficient quenchers; we believe that the high efficiency is the result of fast energy migration, which eventually funnels the energy to the end chromophores in the polymer, effectively leading to quenching by remote energy sinks. The importance of end groups in controlling migration processes had also been recognized

0024-9297/79/2212-1167$01.00/0 

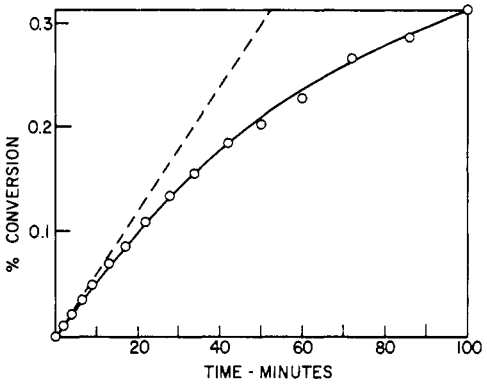


**Figure 1.** Degradation of PPVK as a function of time for polymer sample 4. The percent conversion was calculated as $100S/\lambda_0$ (see glossary, Appendix I).

in the case of poly(1-vinylnaphthalene).[14a]

This paper reports an experimental and theoretical study of the photodegradation of samples of poly(phenyl vinyl ketone) of different chain lengths. The model proposed is based on the one-dimensional random-walk theory[31] and has allowed us to estimate the rate of energy migration in the polymer. In addition, three appendices include a glossary of terms, laser flash photolysis data showing that $\alpha,\beta$-unsaturated carbonyl chromophores are indeed excellent triplet quenchers, and finally a series of numerical calculations showing the way in which the composition of the polymer and the nature of the different fragments change as the reaction proceeds.

## Results

The progress of the reaction was monitored following the change in viscosity of benzene solutions (at 30 °C) of polymer samples. The samples were contained in a viscosimeter, modified so that the solutions could be degassed and irradiated in situ. The value of the number of bonds cleaved per initial macromolecule, $S$, was calculated from[23]

$$S = ([\eta]_0/[\eta])^{1/0.84} - 1 \quad (2)$$

The intrinsic viscosity $[\eta]$ was obtained from:

$$\eta_{sp}/c = [\eta] + Kc[\eta]^2 \quad (3)$$

Molecular weights, $W$, were estimated according to

$$[\eta] = 2.82 \times 10^{-5} W^{0.84} \quad (4)$$

Testing of the ideas involved in the model to be described below requires the careful measurement of the deviation from linearity in plots of conversion vs. time. The flow time for each sample was measured several times, and the average and standard deviation $\sigma$ were then calculated. Typically, $\sigma$ was less than 1% of the difference in flow time between the solvent and the polymer solution. Only when the molecular weight was below 60 000 was it difficult to achieve this reproducibility, and in a few of these cases $\sigma$ might reach 3% of the difference mentioned above.

The preparation of the polymer samples proved to be critical in order to obtain reproducible results. All of the samples used in our experiments were prepared from freshly double distilled monomer by using azobis(isobutyronitrile) or di-*tert*-butyl peroxide as initiator, depending upon the temperature at which the polymerization was carried out. Conversions during the polymerization were usually around 10–15% and always below 20%; typically a 1:2 monomer–benzene mixture was employed. The samples were then precipitated with methanol and dissolved in benzene; the process was repeated ten times. The samples were then freeze-dried. All of these operations were carried out in a dark room, and the final samples were used within 2 weeks following their preparation. Our results do not indicate any trend with the type of initiator used.

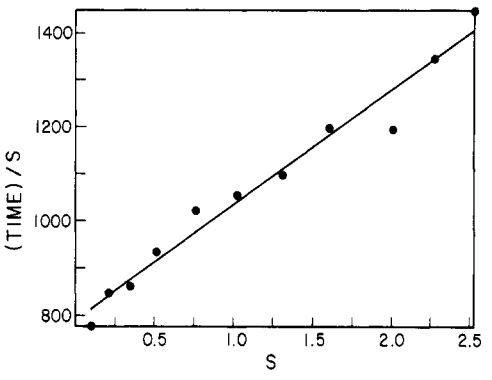


**Figure 2.** Plot of $t/S$ vs. $S$ for polymer sample 6.[34]

Our results are summarized in Table I. All these experiments were carried out with samples containing 0.86 g of polymer per 100 mL of solvent; that is, the actual molar polymer concentration changes, reflecting changes in the molecular weight, but the chromophore concentration, and therefore the optical density of the solutions, remains constant. A series of experiments with more dilute polymer solutions showed the same type of behavior. A study of the initial slopes of plots of conversion vs. time for some of the samples in Table I (samples 2, 6, 7, and 12) led us to estimate $\Phi_{II}^0$, the quantum yield of the type-II process at zero time, as 0.24, in agreement with earlier reports.[20] This inefficiency is not unusual. The type-II process occurs via the intermediacy of biradicals (1) which

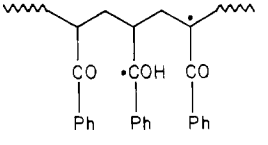


1

can either fragment to yield A and B (reaction 1) or regenerate the parent ketone, in this case PPVK.[32,33] In other words, 0.24 should be regarded as the probability of biradical partition into products.[20]

In order to test the kinetic model described below, it is necessary to evaluate the effective UV dose, $\chi$, defined as $I_a\alpha t/[P]_0$, that is, the intensity of light absorbed times $\alpha$, the efficiency coefficient for the type-II process ($\alpha = 0.24$), times the time divided by the molar polymer concentration. It can be easily shown that at $t = 0$ the limit of the ratio $t/S$ extrapolates to $[P]_0/I_a\alpha$. This extrapolation was carried out from a plot of $t/S$ vs. $S$, which is reasonably linear and facilitates the extrapolation.[34] The doses used in the next section were obtained in this manner; since they eliminate errors due to the actinometry measurements for individual runs, they are independent of the actual value of $\alpha$, and even if intersystem crossing did not occur with unity efficiency, it would be irrelevant. Figure 2 shows a typical $t/S$ vs. $S$ plot.

The UV spectra of fresh and irradiated solutions were for all practical purposes identical, clearly showing that the change in slope of conversion plots is not the result of a change in the absorption characteristics of the solutions.

PPVK phosphoresces at 77 K in a toluene glass with $\lambda(0,0) = 400$ nm, which should be compared with 391 nm

Table I
Fragmentation Data for the Photodegradation of Samples of PPVK in Benzene at 30 °C

| dose (x)[a] | $\eta_{sp}$ | S | dose (x)[a] | $\eta_{sp}$ | S |
|---|---|---|---|---|---|
| Sample 1: $\lambda_0 = 891$; $[P]_0 = 7.17 \times 10^{-5}$ M | | | | | |
| 0.0 | 0.531 | 0.0 | | | |
| 0.10 | 0.478 | 0.11 | 2.28 | 0.269 | 1.04 |
| 0.40 | 0.388 | 0.38 | 3.27 | 0.232 | 1.40 |
| 0.74 | 0.341 | 0.58 | 4.36 | 0.207 | 1.72 |
| 1.19 | 0.314 | 0.73 | 5.54* | 0.186 | 2.06 |
| 1.68 | 0.282 | 0.94 | 6.73* | 0.175 | 2.28 |
| Sample 6: $\lambda_0 = 1036$; $[P]_0 = 6.29 \times 10^{-5}$ M | | | | | |
| 0.0 | 0.616 | 0.0 | 1.37 | 0.312 | 1.02 |
| 0.10 | 0.560 | 0.10 | 1.83 | 0.276 | 1.31 |
| 0.23 | 0.509 | 0.21 | 2.44 | 0.247 | 1.60 |
| 0.38 | 0.459 | 0.35 | 3.05 | 0.216 | 2.01 |
| 0.61 | 0.411 | 0.51 | 3.88 | 0.200 | 2.27 |
| 0.99 | 0.355 | 0.76 | 4.64* | 0.187 | 2.53 |
| Sample 7: $\lambda_0 = 1091$; $[P]_0 = 5.97 \times 10^{-5}$ M | | | | | |
| 0.0 | 0.649 | 0.0 | 1.93 | 0.296 | 1.26 |
| 0.14 | 0.565 | 0.15 | 2.64 | 0.259 | 1.61 |
| 0.29 | 0.510 | 0.27 | 4.07 | 0.192 | 2.62 |
| 0.86 | 0.391 | 0.68 | 5.21* | 0.188 | 2.71 |
| 1.21 | 0.332 | 0.99 | | | |
| Sample 4: $\lambda_0 = 1452$; $[P]_0 = 4.49 \times 10^{-5}$ M | | | | | |
| 0.0 | 0.868 | 0.0 | 2.94 | 0.276 | 2.24 |
| 0.35 | 0.660 | 0.31 | 3.63 | 0.246 | 2.66 |
| 0.56 | 0.575 | 0.50 | 4.32 | 0.231 | 2.92 |
| 0.78 | 0.509 | 0.70 | 5.19 | 0.213 | 3.29 |
| 1.12 | 0.436 | 1.00 | 6.22* | 0.191 | 3.84 |
| 1.47 | 0.391 | 1.23 | 7.44* | 0.181 | 4.13 |
| 1.90 | 0.342 | 1.57 | 8.65* | 0.170 | 4.52 |
| 2.42 | 0.303 | 1.93 | | | |
| Sample 9: $\lambda_0 = 1760$; $[P]_0 = 3.70 \times 10^{-5}$ M | | | | | |
| 0.0 | 1.064 | 0.0 | 6.24 | 0.204 | 4.46 |
| 0.48 | 0.728 | 0.44 | 8.64 | 0.169 | 5.74 |
| 0.96 | 0.572 | 0.83 | 11.04* | 0.148 | 6.82 |
| 1.68 | 0.438 | 1.41 | 13.92* | 0.132 | 7.85 |
| 2.40 | 0.355 | 2.00 | 16.80* | 0.122 | 8.73 |
| 3.36 | 0.298 | 2.61 | 19.68* | 0.112 | 9.68 |
| 4.80 | 0.237 | 3.64 | 24.00* | 0.103 | 10.75 |
| Sample 12: $\lambda_0 = 2008$; $[P]_0 = 3.24 \times 10^{-5}$ M | | | | | |
| 0.0 | 1.225 | 0.0 | 3.59 | 0.355 | 2.42 |
| 0.34 | 0.921 | 0.31 | 4.17 | 0.322 | 2.79 |
| 0.68 | 0.722 | 0.66 | 4.85 | 0.280 | 3.40 |
| 1.07 | 0.609 | 0.96 | 5.62 | 0.260 | 3.77 |
| 1.45 | 0.523 | 1.29 | 6.69 | 0.235 | 4.33 |
| 1.84 | 0.471 | 1.55 | 7.75 | 0.220 | 4.72 |
| 2.23 | 0.423 | 1.85 | 8.92 | 0.199 | 5.39 |
| 2.62 | 0.392 | 2.08 | 10.27 | 0.199 | 5.40 |
| 3.00 | 0.384 | 2.15 | | | |
| Sample 10: $\lambda_0 = 2755$; $[P]_0 = 2.36 \times 10^{-5}$ M | | | | | |
| 0.0 | 1.738 | 0.0 | 5.31 | 0.354 | 3.70 |
| 0.56 | 1.118 | 0.49 | 6.27 | 0.346 | 3.82 |
| 0.88 | 0.934 | 0.77 | 7.24 | 0.301 | 4.59 |
| 1.21 | 0.776 | 1.12 | 8.85 | 0.261 | 5.52 |
| 1.77 | 0.624 | 1.63 | 10.46 | 0.250 | 5.83 |
| 2.41 | 0.534 | 2.07 | 12.06 | 0.226 | 6.62 |
| 3.06 | 0.486 | 2.38 | 13.67 | 0.211 | 7.24 |
| 3.70 | 0.461 | 2.57 | 16.41 | 0.200 | 7.75 |
| 4.34 | 0.414 | 2.99 | 20.43* | 0.172 | 9.35 |
| Sample 13: $\lambda_0 = 2854$; $[P]_0 = 2.28 \times 10^{-5}$ M | | | | | |
| 0.0 | 1.809 | 0.0 | 6.50 | 0.308 | 4.66 |
| 0.49 | 1.147 | 0.51 | 7.15 | 0.293 | 4.96 |
| 0.98 | 0.877 | 0.95 | 7.80 | 0.278 | 5.32 |
| 1.46 | 0.726 | 1.34 | 8.46 | 0.262 | 5.74 |
| 1.95 | 0.615 | 1.76 | 9.43 | 0.246 | 6.21 |
| 2.60 | 0.525 | 2.24 | 10.41 | 0.233 | 6.64 |
| 3.25 | 0.465 | 2.67 | 11.38 | 0.221 | 7.10 |
| 3.90 | 0.420 | 3.08 | 13.25 | 0.194 | 8.36 |
| 4.55 | 0.384 | 3.47 | 14.96* | 0.182 | 9.02 |
| 5.20 | 0.353 | 3.89 | 16.59* | 0.171 | 9.77 |
| 5.85 | 0.328 | 4.29 | 18.54* | 0.164 | 10.26 |
| Sample 2: $\lambda_0 = 2967$; $[P]_0 = 2.20 \times 10^{-5}$ M | | | | | |
| 0.0 | 1.890 | 0.0 | 6.87 | 0.297 | 5.11 |
| 0.34 | 1.362 | 0.34 | 9.16 | 0.250 | 6.36 |
| 0.69 | 1.087 | 0.65 | 11.45 | 0.212 | 7.80 |
| 1.03 | 0.945 | 0.89 | 13.74 | 0.197 | 8.57 |
| 1.37 | 0.773 | 1.29 | 17.18* | 0.175 | 9.87 |
| 2.17 | 0.593 | 1.98 | 20.84* | 0.155 | 11.50 |
| 3.44 | 0.479 | 2.69 | 25.19* | 0.144 | 12.58 |
| 4.58 | 0.380 | 3.70 | | | |

[a] Calculated from the experimental time and the intercept of plots of the type shown in Figure 2. The asterisk denotes values measured under conditions of $W \leq 40\,000$.

for acetophenone and 401 nm for 1,5-diphenyl-1,5-pentanedione (in methylcyclohexane). The result is indicative of a weak interaction between chromophores which still retain the main characteristics of localized excited states.

Finally, examination of fresh and preirradiated samples of PPVK confirms that the rate for the latter is smaller and that the corresponding plot shows less curvature; e.g., Figure 3 shows a plot for two samples of initial molecular weight ~137 000, one of them fresh (number 6) and the other obtained by partial degradation of sample 13 (see Table I) until a molecular weight close to the one given above was obtained.

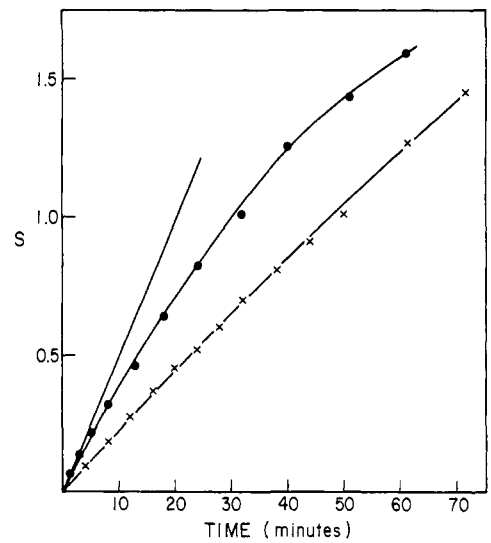


**Figure 3.** Conversion plots for fresh (●) and preirradiated (×) samples of PPVK of approximately matched molecule weight (~137 000).

## Kinetic Model

In order to understand the main features of photodegradation dynamics and also to extract the frequency of excitation migration from our experiments, we have developed a simple kinetic model for the photodegradation of PPVK. The same ideas should be applicable to other polymer systems. Our objective is to obtain the number of bond cleavages (or the number of fragments) as a function of time under conditions of constant light illumination. A distribution function for the fragment size is outside of our scope. Consequently, we assume that a polymer is fragmented into two smaller polymers of equal size at each stage of the degradation with a certain probability which is dependent upon the polymer size and the

number of quenchers in the polymer. The basic processes are then those shown here.

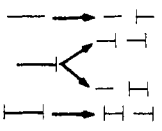

(5a)



(5b)



(5c)

The segments in reaction 5 represent polymers of chain length proportional to their own length, and the perpendicular bar at the end indicates the presence of a quencher group of the type shown in eq 1.

The model described below uses the concept of "stages in the degradation". For every stage, the average size of the polymer decreases to one-half of the previous stage. The initial, nondegraded polymer will be referred to as the first stage. The size of the products of cleavage of first stage polymers will, on average, be one-half of the initial size, and they will be referred to as the second stage. With similar arguments, when we reach, e.g., the fifth stage, the average size of the polymer molecules at this stage will be $^1/_{16}$ of the initial chain length.

The initial polymer with $\lambda_0$ chromophore units contains no quencher and will be designated as the EE-type (shown graphically as —) chain. All of the EE-type polymers can be fragmented with probability 1, when a photon is absorbed. We note at this point that the effective light dose mentioned before already includes the factor $\alpha = 0.24$, taking into consideration the fragmentation to reabstraction ratio for the biradical. The fragmentation of the initial polymer leads to mixture of EE- and EQ-type molecules, where the latter refers to the chain with one quencher on one end (graphically —|). This mixture of EE and EQ with average chain length equal to $\lambda_0/2$ will be referred to as the second stage of degradation. The EQ-type polymers do not necessarily dissociate with probability 1. We shall describe this probability function later. The degradation of second-stage polymers leads to a mixture (third stage) containing EE, EQ, and QQ polymers, where QQ represents a chain with quenchers on both ends. Third-stage polymers will have an average chain length equal to $\lambda_0/4$. The QQ-type polymers have a different probability function from that of the EQ type.

As the degradation progresses, the fragment polymers consist of increasingly complex mixtures of EE, EQ, and QQ types of different lengths. At a certain stage of degradation, the chain lengths for the EQ and QQ types become so short that the probability of their bond cleavages becomes negligible. The EE-type polymers, however, will continue to fragment until the "polymer" consists of a single chromophore.

Before we discuss our kinetic scheme, let us consider the probability function for the type-II reaction as a function of the chain length $\lambda$ for the EQ- and QQ-type polymers. If the probability of finding the excitation initially at some site in the chain is uniform throughout the chain, the survival probability of the excitation for the QQ type can be calculated by the theory of random walk for a loop with a trap.[31] The survival probability at time $t$, $P_s(t)$, is given by,

$$P_s(t) = \exp[-6k_H t/(5 + \lambda^2)] \tag{6}$$

where $k_H$ is the rate of excitation transfer, and $\lambda$ is the chain length. Since $\lambda$ of our interest is of the order of $10^3$ or larger, we shall approximate eq 6 by:

$$P_s(t) \simeq \exp[-6k_H t/\lambda^2] \tag{7}$$

For the EQ-type polymers of chain length $\lambda$, the survival probability can be found simply by replacing $\lambda$ by $2\lambda$ in eq 7.

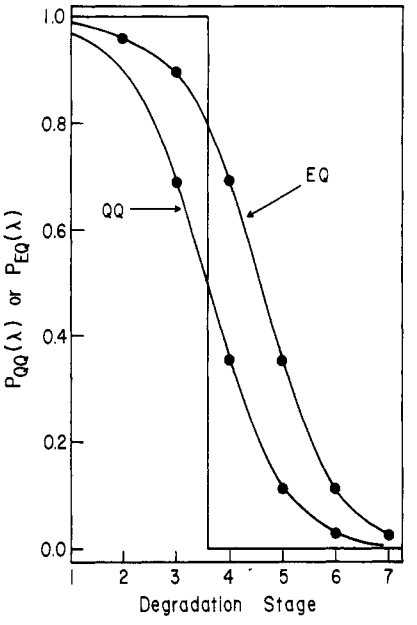


**Figure 4.** Cleavage probability for polymers of the EQ and QQ type for a hypothetical system where $\lambda_0/\lambda_c = 6$.

If $k_{II}$ is the rate constant for the type-II reaction (i.e., fragmentation), the average time required for a bond cleavage is $k_{II}^{-1}$. The probability of bond cleavage for a polymer of the QQ type, $P_{QQ}(\lambda)$, is then given by

$$P_{QQ}(\lambda) = (1 + 6k_H/k_{II}\lambda^2)^{-1} \tag{8}$$

Similarly, for the EQ type,

$$P_{EQ}(\lambda) = (1 + 1.5k_H/k_{II}\lambda^2)^{-1} \tag{9}$$

It is clear from eq 8 and 9 that, for a very large $\lambda$, the probability of dissociation is close to unity; i.e., the effect of quenchers is negligible. As $\lambda$ becomes small, the probability of dissociation becomes smaller. Since the size of $\lambda$ changes by a factor of 2 as the photodegradation progresses to a next stage, $P_{QQ}(\lambda)$ can be taken as equal to unity until $\lambda$ decreases to a critical size, $\lambda_c$.

$$\lambda_c \equiv (6k_H k_{II}^{-1})^{1/2} \tag{10}$$

That is, $\lambda_c$ is the chain length for which a polymer with quencher groups on both ends will have a probability of cleavage of 0.5. When $\lambda < \lambda_c$, the probability of cleavage can be approximated as equal to 0. Figure 4 shows the probability function for a polymer of $\lambda_0/\lambda_c = 6.0$, clearly showing the approximation used. Because of this rapid variation of functions 8 and 9, we approximate them by stepfunctions; namely,

$$P_{QQ}(\lambda) = 1 \text{ for } \lambda > (6k_H k_{II}^{-1})^{1/2}$$
$$P_{QQ}(\lambda) = 0 \text{ for } \lambda \leq (6k_H k_{II}^{-1})^{1/2} \tag{11a}$$

$$P_{EQ}(\lambda) = 1 \text{ for } \lambda > (1.5k_H k_{II}^{-1})^{1/2}$$
$$P_{EQ}(\lambda) = 0 \text{ for } \lambda \leq (1.5k_H k_{II}^{-1})^{1/2} \tag{11b}$$

and for EE polymers

$$P_{EE}(\lambda) \equiv 1 \text{ for } \lambda \geq 2 \tag{11c}$$

The use of the above approximation in terms of the critical size $\lambda_c$ in our kinetic scheme provides an essential simplification of the mathematics involved without sacrificing the physical features of the photodegradation as far as the order of magnitude for the fragmentation efficiency is concerned.

We now proceed to the description of our kinetic scheme. Let $y_i(t)$ be the number of polymers per unit

volume at the $i$th stage of degradation. In this notation, $y_1(0)$ is the concentration of initial polymers at zero time $\{y_1(0) \equiv [P]_0\}$. Since the polymer size at any given stage is one-half of that for the preceeding stage in our approximation, the following conservation law holds at any time.

$$y_1(0) = \sum_{m=1} y_m(t)/2^{m-1} \tag{12}$$

It is convenient to define a variable $\chi$ which is proportional to the absorbed photon dosage,

$$\chi = 0.24 I_a t/[P]_0 \tag{13}$$

where $I_a$ is the intensity of light absorbed, $t$ is the time, and 0.24 is the efficiency factor for the type-II reaction. In terms of this new variable, eq 7 is still valid with $t \rightarrow \chi$, and the kinetic equations are the following:

$$\frac{dy_1(\chi)}{d\chi} = -y_1(\chi)$$

$$\frac{dy_2(\chi)}{d\chi} = 2y_1(\chi) - y_2(\chi)/2$$

$$\frac{dy_3(\chi)}{d\chi} = y_2(\chi) - y_3(\chi)/4$$

$$\vdots$$

$$\frac{dy_n(\chi)}{d\chi} = y_{n-1}(\chi)/2^{n-3} - [y_n(\chi) - y_n^{(3)}(\chi)]/2^{n-1}$$

$$\frac{dy_{n+1}(\chi)}{d\chi} = [y_n(\chi) - y_n^{(3)}(\chi)]/2^{n-2} - [y_{n+1}(\chi) - y_{n+1}^{(2)}(\chi) - y_{n+1}^{(3)}(\chi)]/2^n$$

$$\frac{dy_{n+2}(\chi)}{d\chi} = [y_{n+1}(\chi) - y_{n+1}^{(2)}(\chi) - y_{n+1}^{(3)}(\chi)]/2^{n+1} - [y_{n+2}(\chi) - y_{n+2}^{(2)}(\chi) - y_{n+2}^{(3)}(\chi)]/2^{n+2}$$

$$\vdots \tag{14}$$

The superscripts indicate the type of polymer (1, 2, and 3 for EE, EQ, and QQ, respectively), and the parameters without superscript refer to the total concentration at a given stage. $y_n^{(3)}(\chi)$ is the number of polymers of QQ type which stopped dissociating at the $n$th stage, while $y_{n+1}^{(2)}(\chi)$ is the number of polymers which stop dissociating at the $(n+1)$th stage (these are the EQ type for $n \geq 3$). For example, in the case of Figure 2, $n \equiv 4$.

In writing eq 14, it is assumed that the critical size $\lambda_c$ is smaller than the polymer size up to the $n$th stage so that all types of polymers dissociate with probability 1 until the $n$th stage is reached (see eq 11). At the $n$th stage (for $n \geq 3$), the QQ-type polymers stop dissociating, so that the depletion term at the $n$th stage of eq 14 is proportional to $[y_n(\chi) - y_n^{(3)}(\chi)]$. The factor $2^{n-1}$ comes from the fact that the absorption coefficient of polymers at the $n$th stage is one $(2^{n-1})$th of that for the initial polymer, as a result of the decrease in the number of chromophores per molecule.

Equation 14 is supplemented by the following set of equations:

$$\frac{dy_n^{(3)}(\chi)}{d\chi} = \kappa_n y_{n-1}(\chi) \tag{15}$$

$$\frac{d[y_{n+1}(\chi) - y_{n+1}^{(2)}(\chi) - y_{n+1}^{(3)}(\chi)]}{d\chi} = \kappa_n'[y_n(\chi) - y_n^{(3)}(\chi)] - [y_{n+1}(\chi) - y_{n+1}^{(2)}(\chi) - y_{n+1}^{(3)}(\chi)]/2^n \tag{16}$$

$$\frac{d[y_{n+2}(\chi) - y_{n+2}^{(2)}(\chi) - y_{n+2}^{(3)}(\chi)]}{d\chi} = [y_{n+1}(\chi) - y_{n+1}^{(2)}(\chi) - y_{n+1}^{(3)}(\chi)]/2^n - [y_{n+2}(\chi) - y_{n+2}^{(2)}(\chi) - y_{n+2}^{(3)}(\chi)]/2^{n+1}$$

$$\vdots$$

where $\kappa_n$ and $\kappa_n'$ are determined by the fractions of the EQ- and QQ-type polymers at the $n$th stage. Equations 14–16 and 12 are sufficient to give an explicit expression for the number of polymers at any given $\chi$ (or time).

Let us now focus on a few examples. When $n = 1$, the QQ-type polymers formally stop dissociating at stage 1, and the EQ type stop at stage 2. In practice, this means the QQ type is never formed (since they cannot be produced before the third stage), and the EQ type are photostable and simply accumulate in the system. In this case,

$$\kappa_1 = \kappa_1' = 1 \tag{17}$$

All of the $y_n^{(2)}(\chi)$'s in eq 14 and 16 may be set equal to zero. Using Laplace transforms of these equations, we can easily show that,

$$S(1) \equiv [\sum_m y_m(\chi) - y_1(0)]/y_1(0) = \mathcal{L}^{-1}\left[\frac{1}{u(u+1)} + \frac{1}{2u(u+1)(u+1/2)} + \frac{1}{2^3u(u+1)(u+1/2)(u+1/4)} + \dots\right] \tag{18}$$

where $\mathcal{L}^{-1}$ indicates the Laplace inverse of the following function and $u$ is the Laplace inverse variable of $\chi$. Taking the Laplace inverse of each term in eq 18 and collecting the common exponential terms, we get

$$S(1) = \left(1 - \frac{\gamma}{3}e^{-\chi}\right) + \sum_{n=1}\left[1 - \frac{\gamma}{3}\frac{2^{1+2+3+\dots+n}}{(2-1)(2^2-1)\dots(2^{n-1}-1)}e^{-\chi/2^n}\right] \tag{19}$$

where

$$\gamma = 1 + \sum_{n=1}\frac{(-1)^n}{(2^3-1)(2^4-1)\dots(2^{2+n}-1)} \tag{20}$$

The case of $n = 2$ is physically quite similar; in this case, the QQ type are expected to become photostable at the second stage and the EQ type at the third. Since QQ polymers are formed for the first time at the third stage, both EQ and QQ polymers will stop dissociating at this stage. The only type of photosensitive EQ polymers will be those at the second stage. In this case, we obtain,

$$S(2) = \tfrac{3}{2}S(1) + e^{-\chi} - e^{-\chi/2} \tag{21}$$

Let us now consider the case in which $n = 3$.

$$\kappa_3 = \tfrac{1}{8} \qquad \kappa_3' = \tfrac{5}{28} \tag{22}$$

By applying the Laplace transform technique, it can be shown that:

$$S(3) \equiv [\sum_m y_m(\chi) - y_1(0)]/y_1(0) = \tfrac{5}{2}S(1) - 1 + \tfrac{2}{3}e^{-\chi} + 3e^{-\chi/2} - \tfrac{8}{3}e^{-\chi/4} \tag{23}$$

If $n = 4$,

$$\kappa_4 = {}^3/_{32} \qquad \kappa_4' = {}^9/_{104} \tag{24}$$

and a similar calculation leads to,

$$S(4) = {}^9/_2 S(1) - {}^9/_2 + {}^{53}/_{42}e^{-\chi} + {}^8/_3 e^{-\chi/2} + {}^{20}/_3 e^{-\chi/4} - {}^{128}/_{21}e^{-\chi/8} \tag{25}$$

For a finite number $m$, it is always possible to write $S(m)$ in terms of $S(1)$ and a finite number of exponential functions.

Figure 5 shows plots of $S(1)$–$S(4)$ as functions of $\chi$ together with experimental points for representative polymers (taken from Table I) with different initial chain lengths. Also represented is the case for $m = \infty$.

Within our kinetic scheme, Figure 5 provides the upper and lower bounds of the critical length $\lambda_c$. Equations 26 show these bounds for all of the polymers examined, the first three being the ones shown in Figure 5.

$$\begin{gathered} 742 \sim \lambda_c > 371 \text{ for sample 2} \\ 1452 > \lambda_c \geq 726 \text{ for sample 4} \\ 1036 \geq \lambda_c > 518 \text{ for sample 6} \\ 1091 \geq \lambda_c > 545 \text{ for sample 7} \\ 1004 > \lambda_c > 502 \text{ for sample12} \\ 1427 > \lambda_c \geq 713 \text{ for sample 13} \\ 891 \geq \lambda_c \text{ for sample 1} \\ 880 > \lambda_c > 440 \text{ for sample 9} \end{gathered} \tag{26}$$

That is,

$$\lambda_c \sim 750$$

and using eq 10,

$$k_H k_{II}^{-1} \sim 9.37 \times 10^4 \text{ M}$$

A closer fit of experimental points is possible by discarding the step function approximation (i.e., eq 11). In view of other approximations introduced in our kinetic scheme, such an attempt does not seem justified. However, we have calculated a few cases for different values of $\lambda_0/\lambda_c$, using numerical methods; these are tedious and as a general rule lack the generality of the analytical approach, but they do provide an idea of the way in which the mixtures of EE, EQ, and QQ at different stages in the degradation evolve as a function of time and are explained in some detail in Appendix III.

## Discussion

Energy migration in polymeric systems is not an unexpected phenomenon; the proximity of chromophores in homopolymers makes them good candidates for triplet energy migration, which is only allowed by the exchange mechanism.[3,5,6] A polymer molecule in which electronic excitation migration or hopping takes place clearly resembles a one-dimensional crystal.

Three-dimensional energy migration models usually lead to a critical radius, which is a measure of how far the energy travels during the lifetime of the excited states. In the system considered herein, we have defined an analogous quantity, the critical chain length, $\lambda_c$, which for a polymer of the QQ type should be interpreted as the average number of chromophores "visited" by the excitation during one triplet lifetime ($k_{II}^{-1}$), which in this case is controlled by the Norrish type-II process.

The value of $\lambda_c$ obtained ($\sim$750) indicates that under our experimental conditions, energy migration is considerably more efficient than the same process at 77 K, for which Geuskens et al.[16a] determined a Terenin radius of 26 Å. The difference between the two processes is even larger if one takes into consideration that the triplet lifetime at 77 K should be about $10^5$ times longer than that in fluid solution at room temperature.

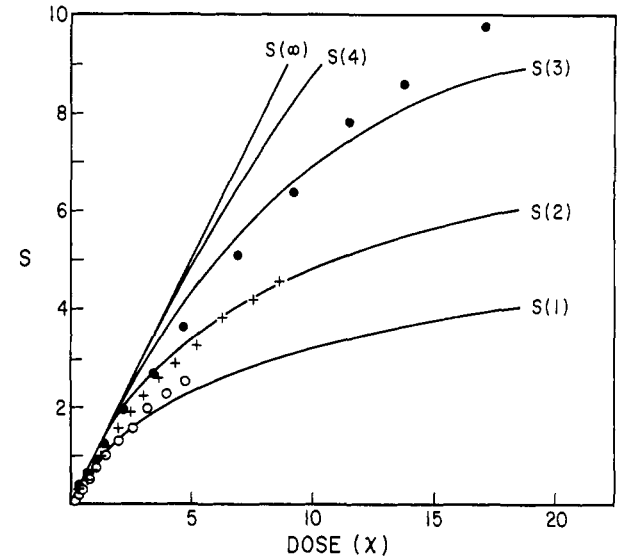


**Figure 5.** Theoretical curves for systems where the degradation of QQ polymers stops at the 1–4 stage and line for $S(\infty)$. Experimental points for polymers 2 (●), 4 (×), and 6 (○).

Most of the previous studies of energy migration in polymers had been carried out in systems where the acceptor, the donor, or both were not part of the polymer molecule, but rather "additives", which act as impurity traps. A problem of concern in all these systems is the possibility of forming aggregates of the additives, which, if present, would inevitably vitiate the results. The system described here has the advantage that the overall process, i.e., excitation, migration, and quenching, is of an intramolecular nature, further, the location of the quencher groups is quite clear, there is no possibility of having sequential quencher groups, and the maximum possible number of quenchers per macromolecule is limited to two.

The chemical changes involved in the process (reaction 1) are also quite clear and well understood.[3,18,32,33] The fact that the reaction does not involve monoradicals is in itself an advantage since it minimizes the possibility of side reactions, and once the two fragments have been formed the reaction is truly irreversible.

The rate constant for energy migration, $k_H$, can be estimated from $\lambda_c$ and the value of $k_{II}$ measured independently. For the latter, we take $k_{II} = 1.7 \times 10^7$ M$^{-1}$ s$^{-1}$; the value has been measured by us, using laser flash photolysis techniques under conditions of "zero conversion" and with polymer samples free of quencher end groups and in the absence of oxygen. Our value of $k_{II}$ is lower than those reported earlier;[20,23,35] however, we find that we can also obtain higher rate values by working with preirradiated samples, which suggests that earlier reports could have employed samples which contained quencher end groups or proceeded to conversions high enough to generate them during the experiment.

Using $\lambda_c$ and $k_{II}$, we obtain $k_H \sim 1.6 \times 10^{12}$ s$^{-1}$; that is *the energy stays roughly 1 ps in each chromophore.* In earlier reports, we have been able to establish that intermolecular triplet energy transfer between aromatic carbonyls of the same type and almost identical triplet energy takes place with rate constants in the neighborhood of $10^9$ M$^{-1}$ s$^{-1}$ in solution at room temperature.[36,37] In intramolecular systems, e.g., the photochemistry of 1,5-diphenyl-2-methyl-1,5-pentanedione[38] or poly(*o*-tolyl vinyl ketone),[39] we had been able to put a lower limit of $10^9$ s$^{-1}$ to the frequency of intramolecular transfer, with some indications that the actual value could be substantially

Table II
Effect of Conversion on the Experimental Quantum Yields of Polymer Degradation

| $\lambda_0^2/\lambda_c^2$ | max $S$ | $\Phi_{obsd}/\Phi_{expect}$ | error, % |
|---|---|---|---|
| 16.0 | 1.0 | 0.98 | −2 |
| 16.0 | 3.0 | 0.93 | −7 |
| 16.0 | 5.0 | 0.86 | −14 |
| 16.0 | 10.0 | 0.72 | −28 |
| 8.3 | 1.0 | 0.97 | −3 |
| 8.3 | 3.0 | 0.89 | −11 |
| 8.3 | 5.0 | 0.81 | −19 |
| 4.1 | 1.0 | 0.95 | −5 |
| 4.1 | 3.0 | 0.83 | −17 |
| 4.1 | 5.0 | 0.73 | −27 |

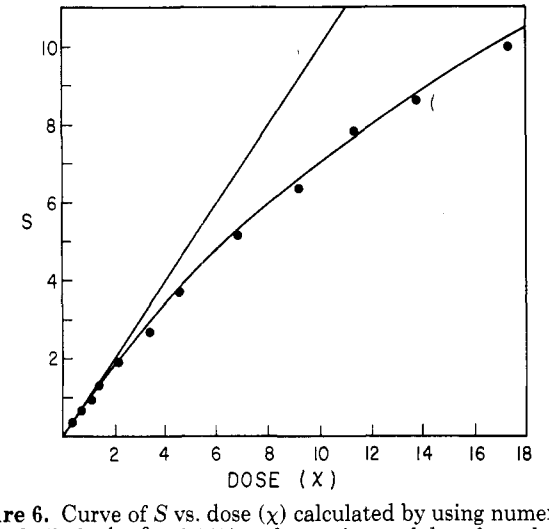


**Figure 6.** Curve of $S$ vs. dose ($\chi$) calculated by using numerical methods ($k_H k_{II}^{-1}\lambda_0^{-2} = 0.025$) and experimental data for polymer 2.

higher than that limit.[40] The value obtained in this work is consistent with those values; nonetheless, it is surprisingly high and must obviously require virtually identical geometrics of the ground state and the lowest triplet state.[41]

It is worth noting that the efficient migration observed is not the result of remote transfers across different sectors of the macromolecule. In recent studies using copolymers of methyl methacrylate–phenyl vinyl ketone–2-vinylnaphthalene, we have shown that transfers of this type take place in a substantially slower time scale, typically hundreds of nanoseconds.[42]

The main feature of the plots in Figure 5 and of the data in Table I is that the curvature is more important for the polymers of shorter chain lengths; this is clearly predicted: the efficiency of quenching by end groups will be higher the shorter the average distance between the original site of excitation and the quencher.

As pointed out above, we have also carried out a series of numerical calculations which are described in some detail in Appendix III. First, given the value of $\lambda_c$ obtained in this work, we estimated the magnitude of the error that would be expected in measurements of $\Phi_{II}^0$ at different conversions and for polymers of different initial size. Some examples are included in Table II, and we believe these can be helpful in establishing what kind of experimental conditions could yield reasonably accurate values in studies of this type. In our experience, the experimental best values are obtained by extrapolation of the $t/S$ vs. $S$ plot to $S \rightarrow 0$, as demonstrated in Figure 2.

For polymer sample 2 (see Table I), we also carried out a numeric fit, shown in Figure 6, where the value of $k_H k_{II}^{-1}$ assumed is $2.1 \times 10^5$ and corresponds to $k_H \sim 3.5 \times 10^{12}$ $s^{-1}$, about twice the value obtained from the analytical treatment. It is interesting to examine the changes predicted in the concentration of the different types of polymer, as the reaction progresses; these are shown in Figures 7–9, also for polymer sample 2. They should be regarded only as semiquantitative information, the main purpose being providing some insight into the main features of the reaction. For the polymers of EE type, we observe that the initial one simply decreases in concentration, while all of the others go through a maximum. For example, for $EE^3$ (subscript = stage of degradation), the maximum is reached for a dose to 4.06. For EQ-type polymers (Figure 8), $EQ^2$ is the first one to appear. Again, if we concentrate on the third stage in the degradation, the maximum for $EQ^3$ is reached for $\chi = 4.69$; we also note

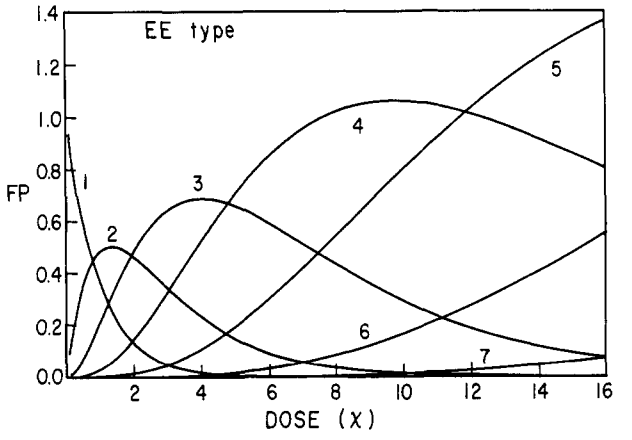


**Figure 7.** Calculated variation of the concentration of EE-type polymers at different stages for $k_H k_{II}^{-1}\lambda_0^{-2} = 0.025$.

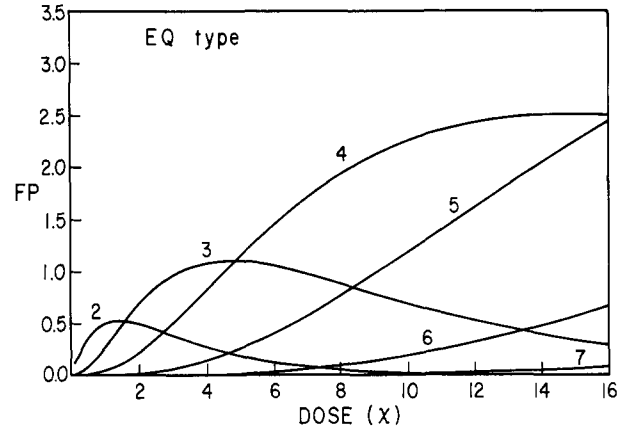


**Figure 8.** The same as Figure 7 but for EQ polymers.

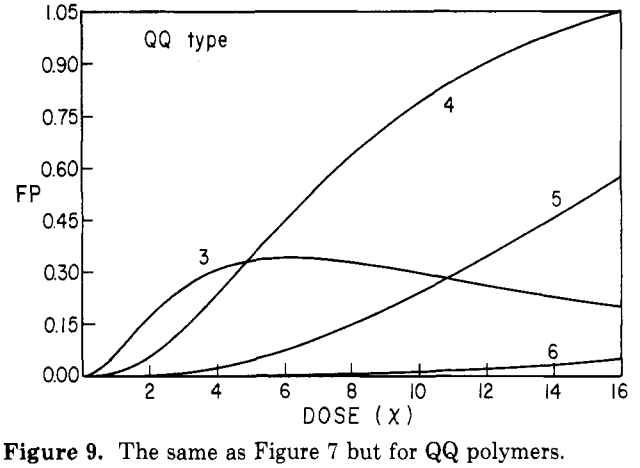


**Figure 9.** The same as Figure 7 but for QQ polymers.

Table III
Calculated Efficiencies of Light Absorption for Polymer Sample 2

| dose (χ) | S | % light absorbed EE | EQ | QQ |
|---|---|---|---|---|
| 0 | 0 | 100 | 0 | 0 |
| 2 | 1.87 | 51 | 44 | 5 |
| 4 | 3.47 | 38 | 51 | 11 |
| 6 | 4.87 | 33 | 53 | 14 |
| 8 | 6.10 | $29_5$ | 53 | $17_5$ |
| 10 | 7.22 | 27 | 54 | 19 |
| 12 | 8.23 | $25_5$ | 54 | $20_5$ |
| 14 | 9.17 | 24 | 55 | 21 |
| 16 | 10.05 | 23 | 55 | 22 |

that the disappearance of EQ[3] is slower than that for EE[3], reflecting that for this particular polymer $P_{EQ}(\lambda_0/4) = 0.68$, while $P_{EE} = 1.0$. The effect is the result of quenching by end groups. For the QQ-type polymers (Figure 9), the first time they are formed is in stage three. Again, we note an increase in the dose value for which the maximum is reached, i.e., $\chi = 6.00$, and an even slower decay reflecting that $P_{QQ}(\lambda_0/4) = 0.34$.

At zero time, 100% of the light is absorbed by EE-type polymers, i.e., the starting material. As the dose increases, the distribution of chromophores changes, and Table III shows the distribution of light-absorbing species as a function of time. As the reaction proceeds, two things happen simultaneously: (i) The amount of light absorbed by EE polymers decreases and (ii) the macromolecules become smaller; as a result the QQ and EQ polymers eventually reach a stage at which their probability of degradation is quite small; the combination of the two effects is of course the cause of the curvature in conversion vs. time plots.

## Conclusion

The photodegradation of poly(phenyl vinyl ketone) leads to the formation of polymer fragments which contain quencher end groups; as a result, the photoreaction shows a self-inhibiting effect, which results from triplet quenching by these unsaturated end groups. The high efficiency of these groups is made possible by the high frequency of triplet energy hopping along the chain. Analysis of the data for polymer samples of different initial chain length leads to the estimation of the critical chain length as 750 units and corresponds to a hopping frequency of $\sim 10^{12}$ s$^{-1}$.

## Experimental Section

**Materials.** Phenyl vinyl ketone was prepared from β-chloropropiophenone following a literature procedure.[43] The fresh monomer was vacuum distilled twice and used for polymer preparation within 24 h. The initiators, azobis(isobutyroritrile) and di-*tert*-butyl peroxide, were used as received. The traces of hydroperoxide which the latter usually contains were purposely not removed. Benzene and methanol were both Aldrich, Gold Label. Propiophenone and valerophenone were also Aldrich products.

Polymerizations were carried out in a 1:2 monomer–benzene mixture (v/v) containing different concentrations of initiators. The samples were maintained in a constant temperature bath long enough to achieve ca. 15% conversion to polymer. In a few cases where polymerization exceeded 20%, the samples were discarded. One sample was prepared by refluxing a 1:2:1 monomer–benzene–di-*tert*-butyl peroxide mixture. The polymers were then precipitated with methanol, washed, and redisolved in benzene; this procedure was repeated ten times. The samples were finally freeze dried from benzene; if the final sample was not enough for three complete conversion curves, they were discarded. All samples were used within 2 weeks following preparation, and all operations related to the preparation, purification, and handling of the polymers were carried out in a dark room. Polymerizations and photodegradations were all carried out under anaerobic conditions.

**Photodegradations.** The progress of the reaction was monitored by measuring the viscosity of the solutions at the end of each irradiation interval. Every measurement was repeated around ten times. The flow times were measured using a Wescan automatic timer (Model 210) combined with a modified viscosimeter which allowed us to deaerate, irradiate, and measure the flow times without any need for sample transfers. The complete unit was immersed in a constant-temperature bath maintained at 30.00 ± 0.02 °C and protected from light, except for the small window used for excitation. A helium/neon laser located nearby was used to ensure that the cell position could be accurately reproduced. The samples were irradiated, using a combination of a Bausch and Lomb 200 W high-pressure mercury lamp and a high-intensity monochromator. All experiments were carried out at 366 nm, and typical light intensities were around $3.3 \times 10^{-7}$ einsteins L$^{-1}$ s$^{-1}$.

**Actinometry.** The Norrish type-II photofragmentation of valerophenone in benzene was used as an actinometer taking Φ(acetophenone) = 0.30.[44] The concentration of acetophenone was determined by gas chromatography, using a Beckman GC-5 instrument equipped with flame ionization detectors and an Apiezon L column.

**Phosphorescence.** Luminescence spectra were recorded in a Spec Fluorolog spectrofluorimeter.

**Laser Photolysis.** The instrument makes use of a Molection UV-400 nitrogen laser. Further details have been given elsewhere.[38]

## Appendix I. Glossary of terms

| | |
|---|---|
| $c$ | polymer concentration in g/100 mL |
| EE | polymer chains containing no quencher groups; if a superscript is given it refers to the stage in the degradation |
| EQ | polymer chains containing only one quencher; see EE for superscript |
| $f_i^{(m)}$ | fraction of the total absorbed light absorbed by polymers of type $m$ (1 = EE, 2 = EQ, 3 = QQ) at degradation stage $i$ |
| $I_a$ | intensity of light absorbed |
| $K$ | Huggins constant[23] |
| $k^0$ | rate constant for triplet decay in the absence of quenchers ($k^0 = \tau_T^{-1}$) |
| $k_{decay}$ | as $k^0$ but in the presence of quenchers |
| $k_Q$ | rate constant for triplet quenching (given in Appendix II for PVK) |
| last $y_i^{(m)}$ | used in the numeric calculations (see Appendix III); the value of $y_i^{(m)}$ is determined after the previous dose increment |
| n | degradation stage at which the QQ polymers stop dissociating, according to equation 11a |
| [P] and $[P]_0$ | molar polymer concentration; at zero time when the subscript 0 is included [P] = 10c/$W$ (refers to all polymers, regardless of stage and type) |
| $P_{EE}$ | probability of cleavage for EE polymers; always equal to 1 |
| $P_{EQ}(\lambda)$ | probability of cleavage for EQ polymers; defined according to eq 9 or 11b |
| $P_{QQ}(\lambda)$ | probability of cleavage for QQ polymers; defined according to eq 8 or 11a |
| PVK | phenyl vinyl ketone |
| PPVK | poly(phenyl vinyl ketone) |
| $P_s(t)$ | survival probability function in a loop with one trap; mathematically equivalent to the case of QQ polymers |
| QQ | polymer chain with quencher groups at both ends; for superscript see EE |
| $S$ | number of bonds cleaved per initial macromolecule; i.e., $S + 1$ is the actual number of fragments |

| | |
|---|---|
| $t$ | time |
| $u$ | Laplace inverse variable to $\chi$ |
| $W$ | molecular weight of polymer (viscosimetry) |
| $y_i^{(m)}$ | concentration of polymers of type $m$ ($m$ = 1, 2, 3 for EE, EQ, and QQ, respectively) at stage $i$; a function of time |
| $\alpha$ | efficiency factor for the type-II reaction; i.e., partition ratio for the biradical and equal to 0.24 in this case (in the case considered herein, $\alpha = \Phi_{II}^0$, assuming the quantum yield of intersystem crossing as unity) |
| $\gamma$ | see equation 20 |
| $\Delta\chi$ | dose increment used for numeric calculations; see appendix III |
| $[\eta]$, $[\eta]_0$ | intrinsic viscosity; the subscript 0 indicates zero time |
| $\eta_{sp}$ | specific viscosity |
| $\kappa_n$, $\kappa_n'$ | fractions of QQ and EQ polymers at the $n$th stage; see equation 16 |
| $\lambda$ | chain length |
| $\lambda_0$ | initial chain length |
| $\lambda_c$ | critical chain length |
| $\Phi_{II}$ | quantum yield of photofragmentation |
| $\chi$ | normalized dose defined as $I_a\alpha t/[P]_0$ and usually determined using plots of the type shown in Figure 2 |

## Appendix II. Determination of the Rate of Triplet Quenching by Phenyl Vinyl Ketone

The validity of the model described herein depends critically upon the quenching properties of end group B in reaction 1; its structure is quite similar to that of phenyl vinyl ketone, and examination of the efficiency of this model molecule should provide some insight into the assumption of efficient quenching mentioned above.

We have carried out a series of experiments in which we measured the rate of quenching of propiophenone triplets by phenyl vinyl ketone. For this we have used laser flash photolysis techniques. We employed a nitrogen laser ($\lambda$ = 337.1 nm, 3 mJ, ~8 ns) for excitation, and the concentration of triplet propiophenone was monitored as a function of time from its T–T absorption.[46] Addition of phenyl vinyl ketone causes an increase of the rate of decay of triplet propiophenone; the experimental rate of decay and the rate constant for quenching are related by

$$k_{decay} = k^0 + k_Q[PVK] \qquad (II\text{-}1)$$

where $k^0$ is the reciprocal of the triplet lifetime. Figure 10 shows a plot according to eq II-1, from which we obtain $k_Q = 1.7 \times 10^9$ M$^{-1}$ s$^{-1}$ at room temperature in benzene solvent. The value is close to diffusion controlled and is consistent with the assumption of very efficient quenching. Wagner[47] has also observed efficient quenching by unsaturated products in the photochemistry of several aromatic ketones.

## Appendix III. Numerical Evaluation of the Polymer Degradation Efficiency

Equations 8 and 9 allow the evaluation of the cleavage probability for any polymer, given the ratio $k_H/\lambda^2 k_{II}$, or alternatively $\lambda/\lambda_c$, since eq 8 and 9 can be easily transformed into

$$P_{QQ}(\lambda) = (1 + \lambda_c^2/\lambda^2)^{-1} \qquad (III\text{-}1)$$

$$P_{EQ}(\lambda) = (1 + \lambda_c^2/4\lambda^2)^{-1} \qquad (III\text{-}2)$$

Our initial condition will be $y_1^{(1)} = 1.0$, and $y_i^{(n)} = 0$ for all other polymers; further, we will allow $i$ to vary between 1 and 9, that is, we will take into consideration 9 degradation stages. Beyond that point (polymer size 1/256 of $\lambda_0$), we will assume that all polymers are photostable; as a result, the model holds only if the ninth degradation level remains basically "empty" throughout the reaction. We have carried out calculations using a step variation of the dose, which if small enough can be approximated to a differential. We have used $\Delta\chi = 0.005$, then we apply eq III-3 to III-5 to the potential 24 species present in the system, starting always at the ninth stage and moving up to the first.

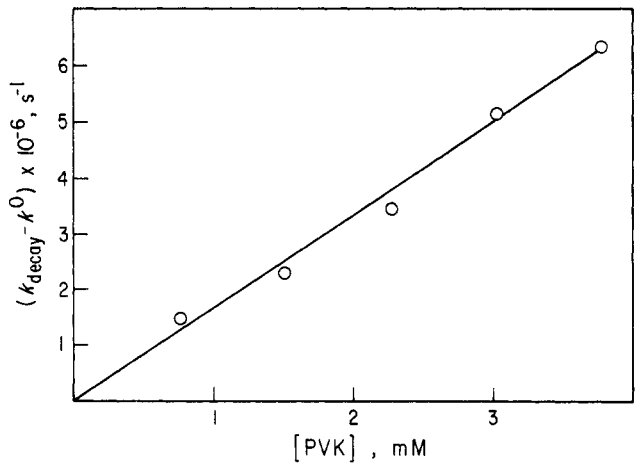


**Figure 10.** Quenching data for the propiophenone–PVK system, according to eq II-1.

$$y_i^{(1)} = \text{last } y_i^{(1)} + \Delta\chi(-f_i^{(1)} + f_{i-1}^{(1)} + \tfrac{1}{2}P_{EQ}(\lambda)f_{i-1}^{(2)}) \qquad (III\text{-}3)$$

$$y_i^{(2)} = \text{last } y_i^{(2)} + \Delta\chi(-P_{EQ}(\lambda)f_i^{(2)} + f_{i-1}^{(1)} + P_{EQ}(\lambda)f_{i-1}^{(2)} + P_{QQ}(\lambda)f_{i-1}^{(3)}) \qquad (III\text{-}4)$$

$$y_i^{(3)} = \text{last } y_i^{(3)} + \Delta\chi(-P_{QQ}(\lambda)f_i^{(3)} + \tfrac{1}{2}P_{EQ}(\lambda)f_{i-1}^{(2)} + P_{QQ}(\lambda)f_{i-1}^{(3)}) \qquad (III\text{-}5)$$

Where the values of $f_i^{(m)}$ are the fraction of light absorbed by any given polymer type and are a function only of its size

$$f_i^{(m)} = \frac{y_i^{(m)}2^{-(i-1)}}{\sum_i\sum_n (y_i^{(m)}2^{-(i-1)})} \qquad (III\text{-}6)$$

The value of $S$, the number of bonds cleaved per initial macromolecule, is then calculated according to

$$S = \frac{\sum_i\sum_n y_i^{(n)}}{y_1^{(1)}} - 1 \qquad (III\text{-}7)$$

The data shown in Figures 6–9 were obtained in this manner and taking

$$k_H/k_{II}\lambda^2 = 0.025 \qquad (III\text{-}8)$$

for polymer sample 2, for which $\lambda_0 = 2967$. Figures 7–9 clearly show that the ninth stage in the degradation does not hold any substantial polymer concentration, even after a dose $\chi = 16$.

## References and Notes

(1) The research described herein was supported by the Office of Basic Energy Sciences of the Department of Energy. This is document NO. NDRL-2018 from the Notre Dame Radiation Laboratory.
(2) Klöpffer, W. *Spectrosc. Lett.* **1978**, *11*, 863–76.
(3) Turro, N. J. *Pure Appl. Chem.* **1977**, *49*, 405–29.
(4) Ranby, B.; Rabek, J. F. "Photodegradation, Photooxidation and Photostabilization of Polymers"; Wiley: London, 1975; Chapter 7.
(5) Terenin, A.; Ermolaev, V. *Trans. Faraday Soc.* **1956**, *52*, 1042–52.

(6) Förster, Th. *Discuss. Faraday Soc.* **1959**, *27*, 7–17.
(7) Voltz, R., *Radiat. Res. Rev.* **1968**, *1*, 301–60 and references therein.
(8) Inokuti, M.; Hirayama, F. *J. Chem. Phys.* **1965**, *43*, 1978–89.
(9) Dexter, D. L. *J. Chem. Phys.* **1953**, *21*, 836–50.
(10) See, e.g., ref 4, Chapter 10.
(11) Turro, N. J.; Steinmetzer, H.-C. *J. Am. Chem. Soc.* **1974**, *96*, 4677–79. *Ibid.* **1974**, *96*, 4679–80.
(12) Turro, N. J.; Kochevar, I. E.; Noguchi, Y.; Chow, M.-F. *J. Am. Chem. Soc.* **1978**, *100*, 3170–77.
(13) Klöpffer, W. *J. Chem. Phys.* **1969**, *50*, 1689–94. *Ibid.* **1969**, *50*, 2337.
(14) (a) Cozzens, R. F.; Fox, R. B. *J. Chem. Phys.* **1969**, *50*, 1532–35. (b) Fox, R. B.; Price, T. R.; Cozzens, R. F. *Ibid.* **1971**, *54*, 79–84. (c) Fox, R. B.; Price, T. R.; Cozzens, R. F.; McDonald, J. R. *Ibid.* **1972**, *57*, 534–41. (d) Fox, R. B.; Price, T. R.; Cozzens, R. F.; McDonald, J. R. *Ibid.* **1972**, *57*, 2284–90.
(15) Fox, R. B.; Cozzens, R. F. *Macromolecules* **1969**, *2*, 182–84.
(16) (a) David, C.; Demarteau, W.; Geuskens, G. *Eur. Polym. J.* **1970**, *6*, 537–45. (b) *Ibid.* **1970**, *6*, 1405–09. (c) David, C.; Putman, N.; Lempereur, M.; Geuskens, G. *Ibid.* **1972**, *8*, 409–15. (d) David, C.; Lempereur, M.; Geuskens, G. *Ibid.* **1972**, *8*, 417–27. (e) David, C.; Demarteau, W.; Geuskens, G. *Ibid.* **1970**, *6*, 1397–1403. (f) David, C.; Naegelen, V.; Piret, W.; Geuskens, G. *Ibid.* **1975**, *11*, 569–74. (g) David, C.; Baeyens-Volant, D.; de Abreau, P. M.; Geuskens, G. *Ibid.* **1977**, *13*, 841–46.
(17) Guillet, J. E. *Polym. Eng. Sci.* **1974**, *14*, 482–86.
(18) Guillet, J. E. *Pure Appl. Chem.* **1977**, *49*, 249–58.
(19) Heskins, M.; Guillet, J. E. *Macromolecules* **1968**, *1*, 97–98.
(20) Golemba, F. J.; Guillet, J. E. *Macromolecules* **1972**, *5*, 212–16.
(21) Dan, E.; Somersall, A. C.; Guillet, J. E. *Macromolecules* **1973**, *6*, 228–35.
(22) Aspler, J. S.; Hoyle, C. E.; Guillet, J. E. *Macromolecules* **1978**, *11*, 925–29.
(23) Lukak, I.; Hrdlovic, P.; Manasek, Z.; Bellus, D. *J. Polym. Sci., Part A-1* **1971**, *9*, 69–80.
(24) Beck, G.; Dobrowolski, G.; Kiwi, J.; Schnabel, W. *Macromolecules* **1975**, *8*, 9–11.
(25) Kiwi, J.; Schnabel, W. *Macromolecules* **1975**, *8*, 430–35. *Ibid.* **1976**, *9*, 468–70.
(26) Faure, J. *Pure Appl. Chem.* **1977**, *49*, 487–94 and references therein.
(27) Beck, G.; Kiwi, J.; Lindenau, D.; Schnabel, W. *Eur. Polym. J.* **1974**, *10*, 1069–75.
(28) Faure, J.; Fouassier, J.-P.; Lougnot, D.-J.; Salvin, R. *Nouv. J. Chem.*, **1977**, *1*, 15–24.
(29) Wissbrum, K. F. *J. Am. Chem. Soc.* **1959**, *81*, 58–62.
(30) Small, R. D. Jr.; Scaiano, J. C. *Macromolecules*, **1978**, *11*, 840–41.
(31) Montroll, E. W. *J. Phys. Soc. Jpn.* **1969**, *26*, 6–10.
(32) Wagner, P. J. *Acc. Chem. Res.* **1971**, *4*, 168–77.
(33) Scaiano, J. C.; Lissi, E. A.; Encinas, M. V. *Rev. Chem. Interm.* **1978**, *2*, 139–96.
(34) We find that plots of $t/S$ vs. $S$ are linear over a wide range of $S$ values; this is of course equivalent to approximating the dependence of $S$ with $t$ with an equation of the type $t \propto S + bS^2$. While empirical, this is a very convenient way of obtaining "zero conversion" parameters.
(35) Faure, J.; Fouassier, J.-P.; Lougnot, D.-J. *J. Photochem.* **1976**, *5*, 13–21.
(36) Encinas, M. V.; Scaiano, J. C. *Chem. Phys. Lett.* **1979**, *63*, 205.
(37) For comparison, the transfer of triplet energy between aliphatic ketones occurs with rate constants of the order of $10^6$ $M^{-1}$ $s^{-1}$. Schuster, G; Turro, N. J. *Tetrahedron Lett.* **1975**, 2261–64.
(38) Bays, J. P.; Encinas, M. V.; Small, R. D., Jr.; Scaiano, J. C. *J. Am. Chem. Soc.*, in press.
(39) Bays, J. P.; Encinas, M. V.; Scaiano, J. C. *Macromolecules* **1979**, *12*, 348–50.
(40) High efficiency for triplet energy transfer has also been reported in the case of benzophenones substituted with nonconjugated naphthalene chromophores (Lamola, A. A.; Leermakers, P. A.; Byers, G. W.; Hammond, G. S. *J. Am. Chem. Soc.* **1965**, *87*, 2322–31), as well as in some 1,6-diketones. Wagner, P. J.; Nakahira, T. *J. Am. Chem. Soc.* **1973**, *95*, 8474.
(41) The difference of nearly three orders of magnitude in the rates of triplet energy migration in aromatic and aliphatic systems has been attributed to differences in the geometries of ground and excited states in the latter.[36,37]
(42) Das, P. K.; Encinas, M. V.; Scaiano, J. C. *J. Photochem.*, submitted.
(43) Freedman, H. H.; Mason, J. P.; Medalia A. I. *J. Org. Chem.* **1958**, *23*, 76–82.
(44) Wagner, P. J.; Keslo, P. A.; Kemppainen, A. E.; McGrath, J. M.; Schott, H. N.; Zepp, R. G. *J. Am. Chem. Soc.* **1972**, *94*, 7506–12.
(45) Small, R. D., Jr.; Scaiano, J. C. *J. Phys. Chem.* **1978**, *82*, 2064–66. *Ibid.* **1978**, *82*, 2662–64.
(46) T–T absorptions were usually monitored at 395 nm. For a more detailed description of similar experiments, see: Encinas, M. V.; Scaiano, J. C. *J. Am. Chem. Soc.* **1979**, *101*, 2146–52.
(47) Wagner, P. J.; Kochevar, I. E.; Kemppainen, A. E. *J. Am. Chem. Soc.* **1972**, *94*, 7489–94.

# Photoresponsive Polymers. Reversible Solution Viscosity Change of Poly(methyl methacrylate) Having Spirobenzopyran Side Groups

**Masahiro Irie,* Akira Menju,[1] and Koichiro Hayashi**

*The Institute of Scientific and Industrial Research, Osaka University, Suita, Osaka, Japan.*
*Received February 27, 1979*

ABSTRACT: Poly(methyl methacrylate) having spirobenzopyran side groups was synthesized in an attempt to construct a photoresponsive polymer, the conformation of which can be photoregulated. Solution viscosity of the polymer was reduced during irradiation and returned to the initial value after removing the light in benzene. The decrease/recovery cycles of the viscosity can be repeated many times without any noticeable fatigue. Solvent effects, as well as spectroscopic studies including laser photolysis, indicate that the photodecrease in viscosity is caused by intramolecular solvation by the methacrylate ester side groups of the polar merocyanines which are produced by irradiation of the spirobenzopyran side groups.

Photoreceptors for photoregulated biological processes seem to consist of photoisomerizable molecules embedded in protein matrices.[2,3] Upon photoexcitation, the molecules undergo geometrical isomerization, which causes changes of conformation of the proteins or the state of assembly in the membranes, leading to nerve excitation or to control of enzymatic activity. Vision, for example, is based on the cis-trans isomerization of retinal.[2]

Photoregulation of the conformation of synthetic polymers has been tried in several systems.[4-7] The basic condition for photoregulation of polymer conformation is to design polymer systems having chromophores capable of transforming light energy into a change in conformation. This condition can be achieved by incorporating the

0024-9297/79/2212-1176$01.00/0 